ESRF	**Experiment title:** **Simultaneous electrical and X-ray characterization of metal-semiconductor contacts**	**Experiment number**: HC-1182
Beamline: ID-11	**Date of experiment**: from: 9th of July 2014 to: 15th of July 2014	**Date of report**:
Shifts: 18	**Local contact(s)**: Jonathan Wright	*Received at ESRF:*

Names and affiliations of applicants (* indicates experimentalists):

Jesper Wallentin*, Markus Osterhoff*, Sarah Hoffmann*, Tim Salditt*

All from: Inst. for X-ray physics, University of Göttingen, Germany

Report:

The long absorption lengths of hard X-rays make them uniquely suitable for *in operando* investigations [1]. Recent advances in the focusing of hard X-rays open up the possibility to investigate functional nanodevices. In this report, we show Bragg scattering measurements of electrically connected semiconductor nanowires (NWs), with about 100 nm real-space resolution. Previously, isolated NWs have been extensively studied [2-4], revealing for instance strain from epitaxial shells [5]. With electrical connections, it would be possible to investigate for instance current-induced lattice heating and piezoelectric displacement fields. In this project we investigated primarily metal-semiconductor contacts, which are technologically important but very difficult to study since they are buried. Experimentally, such measurements require gradually scaling the electric circuit size to similar size of the NWs, while keeping the setup X-ray transparent.

First, single-crystal InP NWs were put on a substrate chip, and individual NWs were contacted using electron beam lithography [6] (Fig. 1A). The chip was then mounted on a chip carrier (white in Fig. 1A) and contacted using wire bonding. For the experiment, a custom-made sample holder with a socket for the chip carrier and contacts for electrical cables was also built. This allowed us to measure several different chips with the same sample holder. The sample holder was mounted on a plate with hole that fit the ID-11

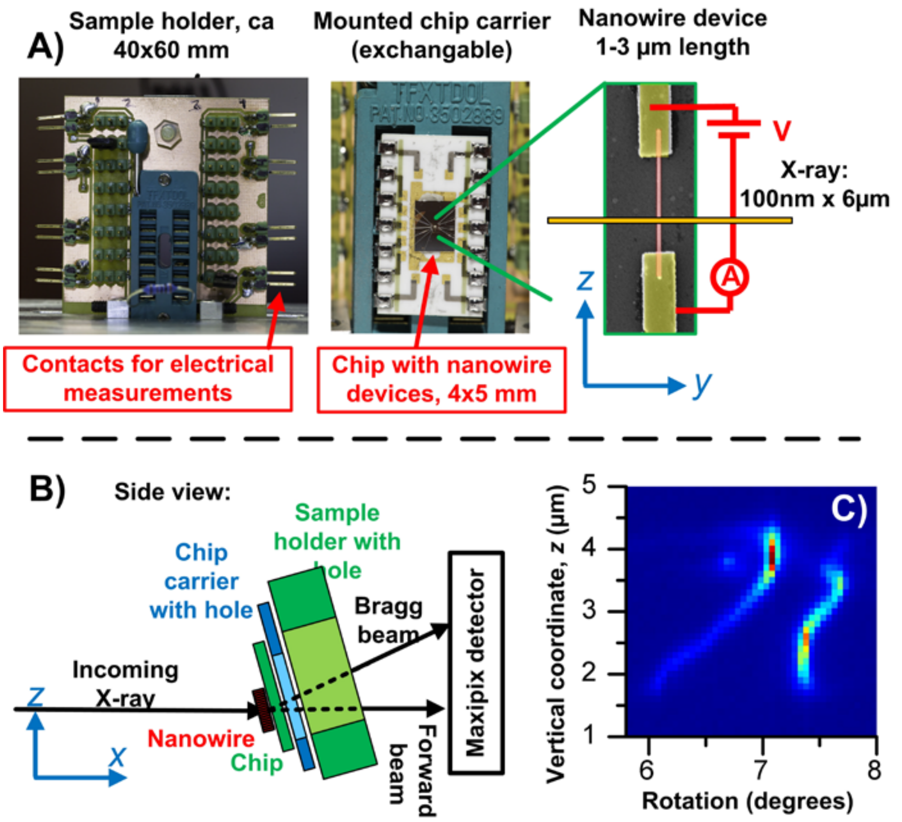

Fig. 1 *A) Sample holder for X-ray scattering measurements of NW devices. B) Drawing of the experiment as seen from the side. C) Map of the Bragg scattering in a strained core-shell NW, as a function of rotation around the y-axis and the vertical coordinate*

piezo stage. Crucially, both the chip carrier as well the sample holder had holes drilled for the X-ray beam. The chip itself is sufficiently X-ray transparent.

The X-ray experiments were performed using a diffractometer at ID-11. The 18 keV beam was focused horizontally with a KB mirror and vertically using compound refractive lenses. The focused beam was highly asymmetric, measuring about 6 µm horizontally and 100 nm vertically. The NW was first rotated around the optical x-axis, to align it vertically. Then, the NW was tilted around the *y*-axis to the Bragg angle of the (111) planes in the NWs. The Bragg scattering was collected with a Maxipix detector (Fig. 1B).

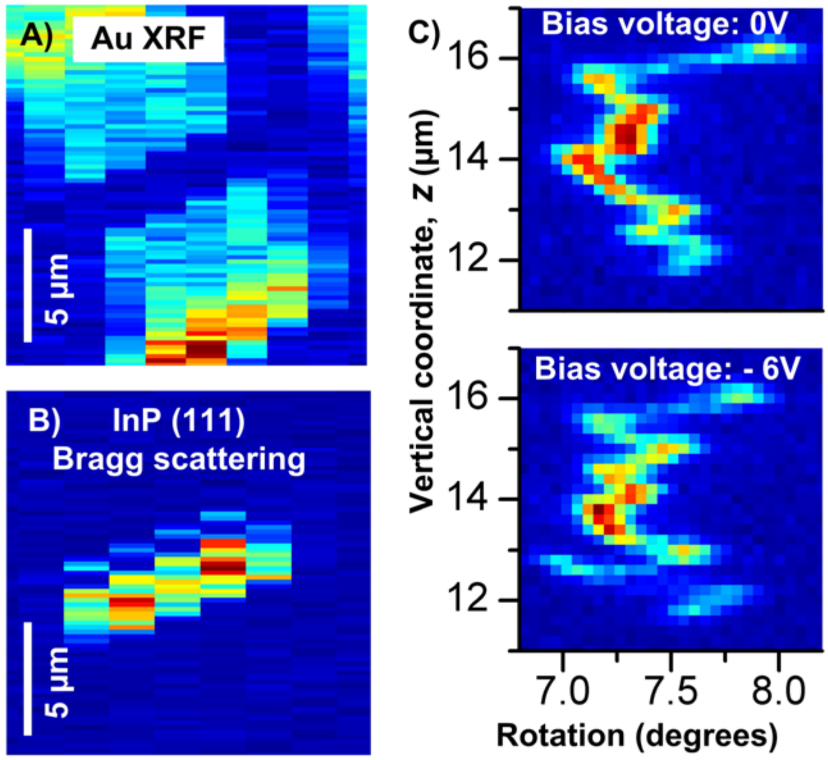

Fig. 2. *A) Map of Au XRF for a NW device. B) Map of Bragg scattering, acquired simultaneously. C) Maps as in Fig. 1C, for the device in Fig. 2A-B, at two different bias voltages. Pronounced differences can be observed at z = 12.5 and 16 µm.*

Each NW was measured by scanning along the NW axis, at slightly different rotations. This created a 2D map of the Bragg intensity as a function of rotation and vertical coordinate (Fig. 1C). We observed strong real-space variations, presumably due to strain and/or bending.

We also used x-ray fluorescence from Au in the contacts to locate the NW devices (Fig. 2A), by making 2D mesh scans with the piezo motors. The XRF made it possible to track and correct for any real-space drift. The device with its 100 nm diameter NW looks broad since the image is a convolution of the 6 µm beam and the object.

After alignment in real and reciprocal space, the device was connected to a voltage source and an amperemeter. We made measurements such as in Fig. 1C at increasingly high bias voltages (*U*), until the device was destroyed and there was no more current through the device. As an example, shown in Fig. 2B, there are clear differences at *U*=0V and *U*=-6V, especially at the ends (contacts). These regions are hidden underneath the metal contacts, which means that they are inaccesible with electron-beam based methods.

Further analysis is under way to understand the results. The plots here show the integrated intensity of the Bragg peak, but by analyzing its center of mass we should be able to distinguish between strain and bending.[7] One possible reason for the observed changes is heating, which would increase the lattice size and shift the Bragg resonance to lower angles. Another possibility is interdiffusion of Au and In, which has been observed ex situ using TEM

In conclusion, we have measured Bragg scattering from single NW devices under bias with about 100 nm real-space resolution. By applying higher voltages, we were able to observe strong lattice changes in the device. The changes were highly localized, which means that they could not have been ientified with a method which averages over the entire device. This is a first demonstration of how *in operando* X-ray measurements can be applied to semiconductor nanodevices.

References

[1] S. Misra, N. Liu, J. Nelson, S. S. Hong, Y. Cui, and M. F. Toney, ACS Nano **6**, 5465 (2012).
[2] M. C. Newton, S. J. Leake, R. Harder, and I. K. Robinson, Nat. Mat. **9**, 120 (2010).
[3] A. Diaz, C. Mocuta, J. Stangl, B. Mandl, C. David, J. Vila-Comamala, V. Chamard, T. H. Metzger, and G. Bauer, Phys. Rev. B **79**, 125324 (2009).
[4] J. Segura-Ruiz, G. Martínez-Criado, M. H. Chu, S. Geburt, and C. Ronning, Nano Lett. **11**, 5322 (2011).
[5] M. Keplinger *et al.*, Nano Lett. **9**, 1877 (2009).
[6] J. Wallentin, M. Ek, L. R. Wallenberg, L. Samuelson, and M. T. Borgström, Nano Lett. **12**, 151 (2011).
[7] T. Etzelstorfer *et al.*, Journal of Synchrotron Radiation **21**, 111 (2014).